

Synthesis and Characterization of New Mixed-Metal Triple-Layered Perovskites, $\text{Na}_2\text{La}_2\text{Ti}_{3-x}\text{Ru}_x\text{O}_{10}$ ($x \leq 1.0$)

John N. Lalena,^{†,§} Alexander U. Falster,[‡] William B. Simmons, Jr.,[‡]
Everett E. Carpenter,^{†,§} Jason Wiggins,[§] Srikanth Hariharan,[§] and
John B. Wiley^{*,†,§}

Departments of Chemistry and Geology and Geophysics and the Advanced Materials Research Institute, University of New Orleans, New Orleans, Louisiana 70148-2820

Received October 14, 1999. Revised Manuscript Received June 12, 2000

The properties of the triple-layered Ruddlesden–Popper oxide $\text{Na}_2\text{La}_2\text{Ti}_3\text{O}_{10}$ have been modified by substituting ruthenium for titanium. Polycrystalline samples of ruthenium-doped sodium lanthanum titanium oxide, $\text{Na}_2\text{La}_2\text{Ti}_{3-x}\text{Ru}_x\text{O}_{10}$ ($x = 0.25, 0.50, 0.75, 1.0$), were prepared by heating the binary oxides at 1000 °C for 24 h under flowing argon. An upper limit to the degree of substitution was found at $x = 1.0$. The phases were structurally characterized by Rietveld analysis of X-ray powder diffraction data. Ruthenium cations are found to exhibit site preferences for the inner-layer octahedral sites, although not to the complete exclusion of the outer layer. A second-order Jahn–Teller effect is thought to influence the site selectively while providing an upper limit to the extent of ruthenium doping. There is spin-glass-like cusp in the magnetic susceptibility of the heavily doped ($x = 1.0$) phase that was not observed with the lighter doping levels. The oxides displayed high electrical resistivity ($7.6 \times 10^3 \leq \rho \leq 3.1 \times 10^6 \Omega \text{ cm}$), which decreased with increasing ruthenium content. The electronic behavior is consistent with that of narrow *d*-band oxides in which there are contributions from both disorder and electron correlation; accordingly, the oxides can be classified as disordered Mott insulators.

Introduction

Electron–electron interactions and electron–phonon interactions in quasi-two-dimensional transport systems have attracted considerable attention since the discovery of high-temperature superconductivity in the layered cuprates. The finding of superconductivity in Sr_2RuO_4 ,¹ in turn, has recently generated interest in the Ruddlesden–Popper (RP)-type ruthenium oxides. These materials resemble the cuprate superconductors, with RuO_2 planes replacing the CuO_2 planes. Cao and co-workers have recently published numerous reports on higher-member single-crystal strontium and calcium-containing ruthenium RP oxides, including: $\text{Sr}_4\text{Ru}_3\text{O}_{10}$,² $\text{Sr}_3\text{Ru}_2\text{O}_7$,³ $\text{Ca}_3\text{Ru}_2\text{O}_7$,⁴ and $(\text{Sr}_{1-x}\text{Ca}_x)_3\text{Ru}_2\text{O}_7$.⁵ All of these oxides are highly correlated, narrow *d*-band systems exhibiting metallic behavior at room temperature.

Several ruthenates in which disorder is present in addition to electron correlation have also been studied. For example, spin-glass behavior has been reported with some oxides containing disordered distributions of

ruthenium cations, such as $\text{Sr}_2\text{FeRuO}_6$,⁶ $\text{Sr}_3\text{FeRuO}_7$,⁷ and $\text{Sr}_4\text{FeRuO}_8$.⁷ In such systems, the interplay between electron correlation energy (U), randomly distributed site energies (W), and one-electron bandwidth governs the magnetic and transport properties.^{8,9} Phase diagrams have been proposed that enable the qualitative electronic behavior to be inferred from the relative strengths of the three parameters.⁹

One possible approach for studying this subject is *filling control*, in which the behavior of a carrier-doped material can be investigated as a function of doping level. Filling control of transition-metal perovskites is usually accomplished by aliovalent substitution of the 12-coordinate cation. In contrast, alloying the octahedral-site cation is avoided because of the risk of reducing the already narrow *d* bandwidth.¹⁰ However, we are interested in observing the manner in which the interplay between correlation and disorder affect the physical properties of a system. Accordingly, we chose to investigate the substitution of the d^0 Ti(IV) with d^4 Ru(IV) $\text{Na}_2\text{La}_2\text{Ti}_3\text{O}_{10}$, an $n = 3$ member of the Ruddlesden–Popper series with distorted outer-layer octahedra.

[†] Department of Chemistry.

[‡] Department of Geology and Geophysics.

[§] The Advanced Materials Research Institute.

(1) Maeno, Y. *Nature* **1994**, *372*, 532.

(2) Cao, G.; McCall, S.; Crow, J. E.; Guertin, R. P. *Phys. Rev. B* **1997**, *56*, R5740.

(3) Cao, G.; McCall, S.; Bolivai, J.; Shepard, M.; Freibert, F.; Henning, P.; Crow, J. E.; Yuen, T. *Phys. Rev. B* **1997**, *54*, 15144.

(4) Cao, G.; McCall, S. C.; Crow, J. E.; Guertin, R. P. *Phys. Rev. Lett.* **1997**, *78*, 1751.

(5) Cao, G.; McCall, S. C.; Crow, J. E.; Guertin, R. P. *Phys. Rev. B* **1997**, *56*, 5387.

(6) Battle, P. D.; Gibb, T. C.; Jones, C. W.; Studer, F. J. *Solid. State Chem.* **1989**, *78*, 281.

(7) Battle, P. D.; Bollen, S. K.; Powell, A. V. J. *Solid State Chem.* **1992**, *99*, 267.

(8) Raychaudhuri, A. K.; Rajeev, K. P.; Srikanth, H.; Gayathri, N. *Phys. Rev. B* **1995**, *51*, 7421.

(9) Zaanen, J.; Sawatzky, G. A.; Allen, J. W. *Phys. Rev. Lett.* **1985**, *55*, 418.

(10) Imada, M.; Fujimori, A.; Tokura, Y. *Rev. Mod. Phys.* **1998**, *70* (4), 1039.

Because of the differences in the radial extent of the 3d and 4d shells, it is conceivable that U and the bandwidth can be tuned with the Ru content. Band structure calculations on ruthenate perovskites have shown strong Ru 4d–O 2p mixing,^{11,12} suggesting that it may be possible to induce metallic transport in the $(\text{Ti}_{1-x}\text{Ru}_x)\text{O}_2$ planes of $\text{Na}_2\text{La}_2\text{Ti}_{3-x}\text{Ru}_x\text{O}_{10}$, by making x very close to 1. This seems plausible because the site preferences, driven by the second-order Jahn–Teller effect of the d^0 titanium, might act to preferentially place the ruthenium in the undistorted central-layer octahedral sites. In any event, the preparation of $\text{Na}_2\text{La}_2\text{Ti}_{3-x}\text{Ru}_x\text{O}_{10}$ constitutes an attempt at carrying out a bandwidth and a filling control study simultaneously. These oxides are thus attractive materials in which to look at the interplay between disorder, correlation, and electronic bandwidth.

Experimental Section

Synthesis. Oxides with compositions $\text{Na}_2\text{La}_2\text{Ti}_{3-x}\text{Ru}_x\text{O}_{10}$ ($x = 0.25, 0.50, 0.75, 1.0$) were prepared by a ceramic method. Appropriate stoichiometric quantities of La_2O_3 (Alfa; 99.9%), TiO_2 (Aldrich; 99.99%), and RuO_2 (Aldrich; 99.9%), were combined with a 30 mol % excess of Na_2CO_3 (Alfa; 99.95%) to give approximately 3.0 g of product. The mixtures were thoroughly ground with an agate mortar and pestle and placed in alumina boats inside a tube furnace at room temperature. The tube was purged with argon (Air Liquide; 99.99%) for 1 h. Afterward, the samples were heated for 24 h at 1000 °C and then allowed to cool under continued argon flow. The samples were subsequently washed with distilled water to remove any excess sodium oxide and then dried in air.

Characterization. Chemical compositions of the reported phases were confirmed by electron probe microanalysis (EPMA) on an ARL-SEM-Q 9-spectrometer instrument with 15–25 kV beam potential, 20 nA beam current, 2 μm beam diameter, and 20–40 s count time/element. The samples were coated with 250 Å carbon.

X-ray powder diffraction data were collected on a Philips X-Pert PW 3020 MPD X-ray diffractometer using $\text{Cu K}\alpha$ radiation ($\lambda = 1.54056 \text{ \AA}$) with a curved graphite single-crystal monochromator. Patterns were recorded by step scanning with 0.02° increments in 2θ over the angular range 10–95°. Crystal structures were analyzed by the Rietveld method using the program PC-Rietveld.¹³ The following agreement indices used were: profile, $R_p = \sum |y_{io} - y_{ic}| / \sum y_{io}$; weighted profile, $R_{wp} = [\sum w_i (y_{io} - y_{ic})^2 / \sum w_i y_{io}^2]^{1/2}$; and goodness of fit (GOF), $\chi^2 = [R_{wp} / R_{exp}]^2$, where $R_{exp} = [(N - P) / \sum w_i y_{io}^2]^{1/2}$, y_{io} and y_{ic} are the observed and calculated intensities, w_i is the weighting factor, N is the total number of y_{io} data when the background is refined, and P is the number of adjusted parameters.

DC magnetic susceptibility measurements on powder samples were made on a Quantum Design MPMS-5S SQUID susceptometer between 2 and 300 K with an applied field of 1000 Oe (zero-field-cooled and field-cooled). Samples were placed in gel capsules inside plastic straws. The magnetic signal of the sample holder was subtracted from the data before correcting for core diamagnetism by Pascal's method.¹⁴

Electrical conductivity was measured on disc-shaped unsintered pressed pellets with a model 2400 Keithley Source

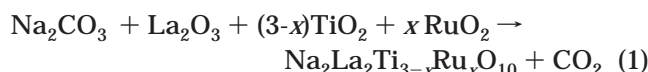
Table 1. Unit Cell Parameters for $\text{Na}_2\text{La}_2\text{Ti}_3\text{O}_{10}$ and the Series $\text{Na}_2\text{La}_2\text{Ti}_{3-x}\text{Ru}_x\text{O}_{10}$

compound	a (Å)	c (Å)	unit cell volume (Å ³)
$\text{Na}_2\text{La}_2\text{Ti}_3\text{O}_{10}$ ²⁰	3.83528(7)	28.5737(7)	420.30(3)
$\text{Na}_2\text{La}_2\text{Ti}_{2.75}\text{Ru}_{0.25}\text{O}_{10}$	3.8412(1)	28.567(1)	421.50(1)
$\text{Na}_2\text{La}_2\text{Ti}_{2.50}\text{Ru}_{0.50}\text{O}_{10}$	3.8464(1)	28.532(1)	422.13(1)
$\text{Na}_2\text{La}_2\text{Ti}_{2.25}\text{Ru}_{0.75}\text{O}_{10}$	3.8560(1)	28.410(1)	422.42(1)
$\text{Na}_2\text{La}_2\text{Ti}_2\text{RuO}_{10}$	3.8606(1)	28.377(1)	422.94(1)

Meter using a square four-probe array technique.¹⁵ Electrical contacts were made by attaching copper wire with silver paste. Data were taken from 298 K down to the temperature at which the sample resistivity exceeded the instrument's measurement capability (~5 M Ω). During data collection, samples were mounted inside a Quantum Design Physical Properties Measurement System (PPMS) for temperature control. The temperature was varied at ~10 °C per minute. Resistance values were converted to resistivity by the method of Wieder.¹⁵

Results

The synthesis of the product phase can be represented as



Because of the loss of ruthenium as the volatile RuO_3 in the presence of oxygen (eq 2),^{16,17} it was necessary to



carry out the reaction under flowing argon. Compounds could then be prepared stoichiometrically, as determined by EPMA, over the compositional range $0 \leq x \leq 1.0$. Efforts to exceed this range, however, were unsuccessful. Samples with higher ruthenium doping levels ($x > 1.0$) always contained an impurity phase. The diffraction pattern of the impurity could be indexed on a cubic unit cell ($a \approx 3.90 \text{ \AA}$) and is most likely a perovskite-related phase such as $\text{La}_{0.67}\text{Ti}_{1-x}\text{Ru}_x\text{O}_3$ or $\text{Na}_y\text{La}_{1-y}\text{Ti}_{1-x}\text{Ru}_x\text{O}_3$. Attempts to prepare the $x = 3$ compound, i.e., $\text{Na}_2\text{La}_2\text{Ru}_3\text{O}_{10}$, resulted in the exclusive formation of this cubic phase.

Unit cell parameters for the set of compounds are presented in Table 1. Volumes are found to increase with increasing ruthenium content (x) predominately through an expansion of a ; c contracts as x increases (Table 1). Rietveld analysis was carried out on each of the four samples. A representative refined X-ray powder diffraction pattern, $x = 0.75$, is shown in Figure 1. It is known that ruthenates can adopt the Ruddlesden–Popper structure^{2–5,7,18} and that six-coordinate Ru^{4+} (0.76 Å) and Ti^{4+} (0.745 Å) ions are similar in size,¹⁹ thus, the positional parameters reported by Toda et al.²⁰ for the parent $\text{Na}_2\text{La}_2\text{Ti}_3\text{O}_{10}$ with the tetragonal space

(11) (a) Singh, D. J. *J. Appl. Phys.* **1996**, *79*, 4818. (b) Allen, P. B.; Berger, H.; Chauvet, O.; Forro, L.; Jarlborg, T.; Junod, A.; Revaz, B.; Santi, G. *Phys. Rev. B* **1996**, *53*, 4393.

(12) (a) Oguchi, T. *Phys. Rev. B* **1995**, *51*, 1385. (b) Singh, D. J. *Phys. Rev. B* **1995**, *52*, 1358.

(13) PC-Rietveld, ver 1.1c, based on code by (a) Wiles, D. B.; Young, R. A. *J. Appl. Crystallogr.* **1981**, *14*, 149. (b) Howard, C. J.; Hill, R. J. *AAEC Rep.* **1986**, No. M112. (c) Fischer, R. X.; Lengauer, C.; Tillmanns, E.; Ensink, R. J.; Reiss, C. A.; Fanter, E. J. *Mater. Sci. Forum* **1993**, *133*, 287.

(14) O'Connor, C. J. *Prog. Inorg. Chem.* **1982**, *29*, 203.

(15) Wieder, H. H. *Laboratory Notes on Electrical and Galvanomagnetic Measurements*; Elsevier: Amsterdam, 1979.

(16) Nikol'skii, A. B.; Ryabov, A. N. *Russ. J. Inorg. Chem.* **1965**, *10*, 1.

(17) Schäfer, von H.; Tebben, A.; Gerhardt, W. *Z. Anorg. Allg. Chem.* **1963**, *321*, 41.

(18) Brandow, B. H. *J. Solid State Chem.* **1975**, *12*, 397.

(19) Shannon, R. D.; Prewitt, C. T. *Acta Crystallogr.* **1969**, *B25*, 925.

(20) Toda, K.; Kameo, Y.; Fujimoto, M.; Sato, M. *J. Ceram. Soc. Jpn.* **1994**, *102*, 737.

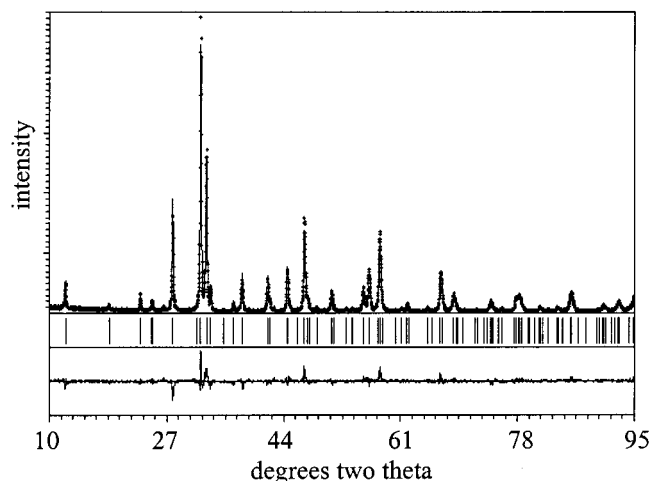


Figure 1. Representative X-ray powder diffraction pattern; $x = 0.75$ from the series $\text{Na}_2\text{La}_2\text{Ti}_{3-x}\text{Ru}_x\text{O}_{10}$.

group $I4/mmm$, were used as a starting model. For all cases, a total of 35 parameters were refined for 89 reflections using a pseudo-Voigt profile function. The background was fit to a six-term polynomial. Individual isotropic temperature factors, B (\AA^2), were used to describe the thermal motion of the atoms. An acceptable temperature factor for the equatorial oxygen of the inner octahedral layer, O(1), was obtained by allowing relaxation off the (100) mirror plane; a recent neutron diffraction study has revealed similar octahedral rotation in $\text{Na}_2\text{La}_2\text{Ti}_3\text{O}_{10}$.²¹ All the temperature factors except the one associated with the bridging oxygen atom, O(2), could be refined. This atom took on negative values so it was therefore necessary to fix it at 1.0 throughout the refinement. Refined positional and thermal parameters are listed in Table 2. Figure 2 illustrates the general location of the atoms within the triple-layered perovskite block. Selected bond distances and angles are presented in Table 3. The distribution of titanium and ruthenium between the two crystallographically distinct octahedral sites was also refined subject to the constraint imposed by the chemical composition of each phase. A clear site preference, although not exclusive, is observed. The percentage of ruthenium distributed between the inner and outer octahedral layers is given in Table 4.

The temperature-dependent molar magnetic susceptibilities of the $x = 0.25, 0.50, 0.75$ samples are shown in Figure 3a. Curie plots of these data exhibit a deviation from linearity (Figure 3b) even at high temperatures (>125 K). For the $x = 1.00$ phase, both field-cooled (FC) and zero-field-cooled (ZFC) temperature-dependent molar magnetic susceptibility are presented in Figure 4 with inverse susceptibility (ZFC only). This compound shows a spin-glass-like cusp in the ZFC data not observed in the other phases. There is also an increase in the susceptibility below the cusp (<10 K). Efforts to fit data for all the samples above 125 K to the Curie-Weiss law were not successful, even when including a temperature independent paramagnetic (TIP) term. Comparison of room-temperature susceptibilities, 0.00106, 0.00155, 0.00203, and 0.00247 for $x =$

Table 2. Atomic and Thermal Parameters for the Series $\text{Na}_2\text{La}_2\text{Ti}_{3-x}\text{Ru}_x\text{O}_{10}$

atom	site	$x = 0.25$	$x = 0.50$	$x = 0.75$	$x = 1.0$
Na^a	z	0.2888(2)	0.2892(3)	0.2899(3)	0.2894(2)
	B (\AA^2)	0.8(1)	0.6(3)	0.9(4)	0.5(2)
	occ	1	1	1	1
La^a	z	0.42456(5)	0.42456(4)	0.42513(5)	0.42502(4)
	B (\AA^2)	1.15(7)	0.7(2)	2.1(3)	0.8(2)
	occ	1	1	1	1
$\text{Ru}(1)^a$	z	0	0	0	0
	B (\AA^2)	0.8(1)	0.3(2)	0.6(3)	0.5(1)
	occ	0.160(6)	0.342(6)	0.454(6)	0.637(5)
$\text{Ti}(1)^a$	z	0	0	0	0
	B (\AA^2)	0.8(1)	0.3(2)	0.6(3)	0.5(1)
	occ	0.839(6)	0.657(6)	0.545(6)	0.362(5)
$\text{Ru}(2)^a$	z	0.1489(1)	0.1482(1)	0.1482(1)	0.14737(8)
	B (\AA^2)	0.26(8)	0.1(2)	0.5(3)	0.1(1)
	occ	0.044(3)	0.078(3)	0.148(3)	0.181(2)
$\text{Ti}(2)^a$	z	0.1489(1)	0.1482(1)	0.1482(1)	0.14737(8)
	B (\AA^2)	0.26(8)	0.1(2)	0.5(3)	0.1(1)
	occ	0.955(3)	0.921(3)	0.852(3)	0.818(2)
O(1)	x	0.097(4)	0.112(3)	0.101(3)	0.120(3)
	y	0.5	0.5	0.5	0.5
	z	0	0	0	0
	B (\AA^2)	3.5(6)	2.1(5)	1.0(5)	0.4(3)
O(2) ^a	occ	0.5	0.5	0.5	0.5
	z	0.0653(3)	0.0669(3)	0.0658(4)	0.0640(3)
	B (\AA^2)	1.0	1.0	1.0	1.0
O(3) ^b	occ	1	1	1	1
	y	0.5	0.5	0.5	0.5
	z	0.1355(2)	0.1354(2)	0.1350(3)	0.1347(2)
O(4) ^a	B (\AA^2)	1.1(2)	0.7(3)	2.2(4)	1.5(2)
	occ	1	1	1	1
	z	0.2103(4)	0.2088(4)	0.2150(6)	0.2108(4)
	B (\AA^2)	2.7(2)	1.2(4)	4.9(5)	3.8(2)
	occ	1	1	1	1
R_{wp}		0.1347	0.1191	0.1226	0.1377
R_p		0.0968	0.0874	0.0907	0.1061
GOF (χ^2)		1.81	1.74	1.88	1.87

^a $x = y = 0$. ^b $x = 0$.

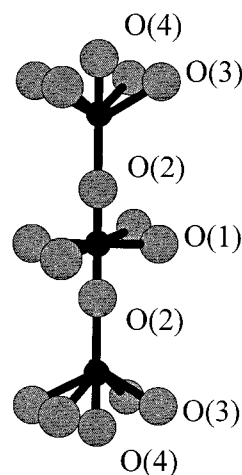


Figure 2. Oxygen coordination around titanium/ruthenium in $\text{Na}_2\text{La}_2\text{Ti}_{3-x}\text{Ru}_x\text{O}_{10}$.

0.25, 0.50, 0.75, and 1.00, respectively, do show a linear increase in susceptibility as a function of ruthenium content.

The temperature dependence of the electrical resistivity (ρ) was measured for each phase. All of the samples were nonmetallic ($d\rho/dT < 0$). There were no indications of a metal-nonmetal transition at any temperature. The room-temperature resistivities of the samples were very high but decreased with increasing ruthenium content. Table 5 lists the room-temperature values. Plots of \ln

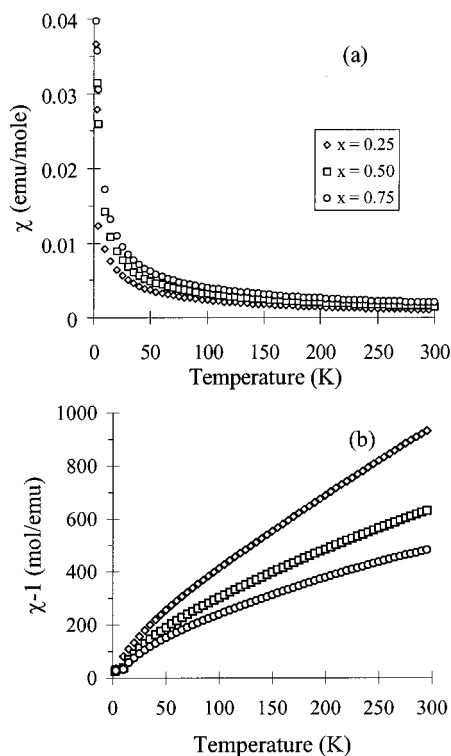
(21) Wright, A. J.; Greaves, C. J. *Mater. Chem.* **1996**, 6 (11), 1823.

Table 3. Selected Bond Distances (Å) and Angles (deg) for the Series $\text{Na}_2\text{La}_2\text{Ti}_{3-x}\text{Ru}_x\text{O}_{10}$

	$x = 0^{20}$	$x = 0.25$	$x = 0.50$	$x = 0.75$	$x = 1.0$
Ti/Ru(1)–O(1)	1.918(0)	1.956(3)	1.971(3)	1.968(2)	1.986(2)
Ti/Ru(1)–O(2)	1.85(4)	1.86(1)	1.90(1)	1.86(1)	1.818(8)
Ti/Ru(2)–O(2)	2.41(4)	2.38(1)	2.32(1)	2.34(1)	2.365(8)
Ti/Ru(2)–O(3)	1.951(5)	1.959(1)	1.957(1)	1.964(1)	1.964(1)
Ti/Ru(2)–O(4)	1.73(4)	1.75(1)	1.73(1)	1.89(1)	1.80(1)
Ti/Ru(1)–Ti/Ru(2)	4.26(7)	4.255(3)	4.229(3)	4.213(3)	4.184(2)
O(1)–Ti/Ru(1)–O(2)	90.0	90.0	90.0	90.0	90.0
O(2)–Ti/Ru(2)–O(3)	79.4(8)	78.5(2)	79.2(2)	78.9(2)	79.4(1)

Table 4. Percent Ruthenium in Inner and Outer Octahedral Layers of $\text{Na}_2\text{La}_2\text{Ti}_{3-x}\text{Ru}_x\text{O}_{10}$ As Determined from Rietveld Analysis

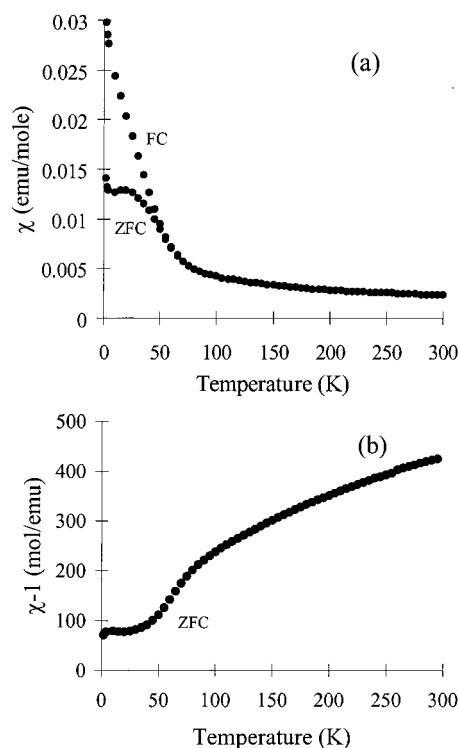
site	$x = 0.25$	$x = 0.50$	$x = 0.75$	$x = 1.0$
2a (inner layer)	16.0(6)	34.2(6)	45.4(6)	63.7(5)
4e (outer layer)	4.4(3)	7.8(3)	14.8(3)	18.1(2)

**Figure 3.** (a) Temperature dependence of the FC molar magnetic susceptibility for $\text{Na}_2\text{La}_2\text{Ti}_{3-x}\text{Ru}_x\text{O}_{10}$ ($x = 0.25, 0.50, 0.75$) samples and (b) inverse susceptibility for $x = 0.25, 0.50, 0.75$ samples.

(ρ) versus $1/T$ were nonlinear while those of $\ln(\rho)$ versus $T^{-1/2}$, $T^{-1/3}$, and $T^{-1/4}$ were all linear. Figure 5 shows the series of plots for the $T^{-1/4}$ behavior.

Discussion

It has been shown that ruthenium can be substituted for titanium in the triple-layer RP oxide $\text{Na}_2\text{La}_2\text{Ti}_3\text{O}_{10}$. The titanium cations in the outer-layer octahedra of $\text{Na}_2\text{La}_2\text{Ti}_3\text{O}_{10}$ exhibit out-of-center displacements due to electrostatic forces.^{20,21} These arise from oppositely charged LaO^+ and NaO^- layers on adjacent sides of the plane containing the metal and equatorial oxygens. The central layer octahedra, on the other hand, are undistorted. In accordance with the second-order Jahn–Teller effect, octahedrally coordinated transition-metal cations with high outer d electron counts are not typically found to exhibit out-of-center distortions.^{22–26} Therefore, it was

**Figure 4.** (a) Temperature dependence of the FC and ZFC molar magnetic susceptibility for $\text{Na}_2\text{La}_2\text{Ti}_{3-x}\text{Ru}_x\text{O}_{10}$ ($x = 1.0$) sample and (b) inverse susceptibility.**Table 5. Room-Temperature Resistivity Values for $\text{Na}_2\text{La}_2\text{Ti}_{3-x}\text{Ru}_x\text{O}_{10}$**

compound	resistivity (Ω cm)
$\text{Na}_2\text{La}_2\text{Ti}_{2.75}\text{Ru}_{0.25}\text{O}_{10}$	3.1×10^6
$\text{Na}_2\text{La}_2\text{Ti}_{2.50}\text{Ru}_{0.50}\text{O}_{10}$	4.4×10^5
$\text{Na}_2\text{La}_2\text{Ti}_{2.25}\text{Ru}_{0.75}\text{O}_{10}$	2.7×10^5
$\text{Na}_2\text{La}_2\text{Ti}_2\text{RuO}_{10}$	7.6×10^3

expected that the non- d^0 ruthenium atoms would exhibit some preference for the inner-layer octahedral sites. Refinements clearly show that ruthenium has a site preference for the inner layer, although a fraction of the metal ions were found in the outer one.

This distribution results in some interesting effects on the compounds structure relative to the parent. The radius of ruthenium (0.76 Å) in a six-coordinate site is only slightly larger than titanium (0.745 Å) so one might simply expect an isotropic expansion. However, the unit cell expansion with increased ruthenium content is

(22) Kunz, M.; Brown, D. *J. Solid State Chem.* **1995**, *115*, 395.

(23) Pearson, R. G. *J. Am. Chem. Soc.* **1969**, *91*, 4947.

(24) Wheeler, R. A.; Whangbo, M.-H.; Hughbanks, T.; Hoffmann, R.; Burdett, J. K.; Albright, T. A. *J. Am. Chem. Soc.* **1986**, *108*, 2222.

(25) Kang, S. K.; Tang, H.; Albright, T. A. *J. Am. Chem. Soc.* **1993**, *115*, 1971.

(26) Bhuvanesh, N. S. P.; Gopalakrishnan, J. *J. Mater. Chem.* **1997**, *7*, 2297.

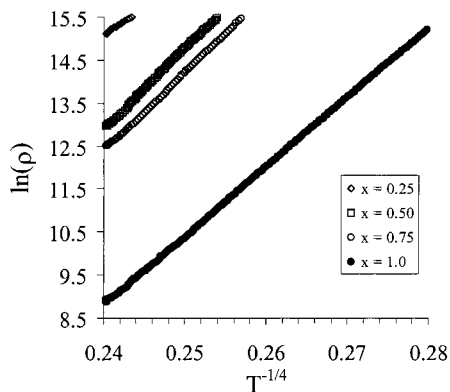


Figure 5. $\ln(\rho)$ versus $T^{-1/4}$ in the series $\text{Na}_2\text{La}_2\text{Ti}_{3-x}\text{Ru}_x\text{O}_{10}$ for $x = 0.25, 0.50, 0.75,$ and 1.0 .

anisotropic (Table 1) in that a increases as c decreases. This is likely an effect of ruthenium in the outer layer working to suppress the out-of-center distortion of this site. Because of the poor X-ray scattering ability of oxygens, their positions are not that reliable. A more dependable measure of the distortion in the outer octahedral layers is then the average metal–metal distance between the inner and outer layers. This distance decreases with increasing ruthenium content (Table 3), corresponding to a decrease in the average out-of-center displacement of the transition-metal cations in the outer-layer octahedra, correspondingly there is an increase in a to offset this effect.

A related phenomenon is likely the stability window for these compounds. We can only prepare $\text{Na}_2\text{La}_2\text{Ti}_{3-x}\text{Ru}_x\text{O}_{10}$ in the range $0 \leq x \leq 1.0$. Presumably, titanium's second-order Jahn–Teller effect is the origin of ruthenium's preference for the undistorted octahedral sites and this effectively places an upper limit on the ruthenium content that can be attained.

The second-order effect is apparently too weak to drive all the ruthenium into the central-layer octahedral sites, thus all the compounds are cation-disordered phases. This does result in some interesting magnetic effects in the $x = 1.00$ phase. The cusp below 50 K in the ZFC magnetic susceptibility of the $x = 1.0$ sample (Figure 4) is characteristic of the spin glass state found in many disordered magnetic systems. Similar transitions have recently been reported in nonperovskite (pyrochlore) ruthenium(IV) compounds.²⁷ This behavior was not observed in the $x = 0.25, 0.50,$ and 0.75 samples. A spin-glass transition might be expected for a geometrically frustrated lattice or for frustrated magnetic interactions. Normally, there is no ambiguity in the sign of the exchange coupling between a pair of Ru^{4+} ions for a 180° cation–anion–cation interaction. However, the oxygen displacements in the outer-layer octahedra associated with the out-of-center distortion could possibly perturb the superexchange interactions. Ferromagnetic exchange interactions would be expected to become more important as the Ru–O–Ru bond angle deviates from 180° .²⁸ Any octahedral rotation or tilting

that may be present could also frustrate the spin coupling. Unfortunately, we were not able to precisely locate the oxygen atoms to our complete satisfaction. Furthermore, given the layered nature of these oxides, it may have been possible to acquire more accurate locations for the octahedral-site cations had we been able to use anisotropic temperature factors to describe the thermal motion of the atoms, however, this was prohibited by the quality of our X-ray data set.

An unusual feature to the magnetic susceptibility of the $x = 1.0$ phase is the infinite or very large susceptibility below the ZFC peak near absolute zero. We believe this behavior can be explained by Simpson's amorphous antiferromagnet model.²⁹ Besides the interactions between neighboring octahedral-site ruthenium cations, it is possible that a fraction of the rutheniums are surrounded by nonmagnetic octahedral-site cations (titanium). These isolated ruthenium atoms will behave as paramagnetic centers swamping out any antiferromagnetic coupling at low temperatures. The more magnetically dilute $x = 0.25, 0.50, 0.75$ systems then are characteristically different from those in which most of the ruthenium atoms interact with at least one neighbor. Amorphous antiferromagnetism has been reported in many magnetic systems, including some disordered oxides.^{30,31}

Each sample displayed a high electrical resistivity. Although the compound with the highest ruthenium content showed the lowest resistivity, no transition to metallic behavior was observed as a function of composition. The simple perovskite, $\text{SrTi}_{1-x}\text{Ru}_x\text{O}_3$, is known to demonstrate metallic conductivity at a composition of $x \approx 0.5$.³² Apparently for metallic behavior to occur in a layered compound like $\text{Na}_2\text{La}_2\text{Ti}_2\text{RuO}_{10}$, where conduction is expected to be predominately in the inner octahedral layer, these values need to exceed 64% ruthenium in the inner layer; at least 36% of the inner octahedral site is Ti 3d character, implying that for an itinerant electron both the Ti 3d–O 2p π mixing and the 3d contribution to the average intrastate correlation energy will be important. The 3d correlation energy will be large in comparison to the 4d energy.³³ Furthermore, the observed expansion of the a lattice parameter and larger (Ti/Ru)–O bond distances, relative to that for $\text{Na}_2\text{La}_2\text{Ti}_3\text{O}_{10}$, suggests poorer Ti–O mixing, and hence narrow overall 3d/4d bandwidth. Electron correlation would be expected to dominate band-structure effects in such a system. As the ruthenium content increases, the bandwidth becomes broader because of increasing 4d character. Likewise, the correlation effects become weaker and the resistivity decreases.

Summary

Consideration of the electrical and magnetic data for $\text{Na}_2\text{La}_2\text{Ti}_{3-x}\text{Ru}_x\text{O}_{10}$ leads us to conclude that disorder and correlation both play important roles in controlling the magnetic and transport properties of these oxides.

(29) Simpson, A. W. *Phys. Status Solidi* **1970**, *40*, 207.

(30) Walstedt, R. E.; Kummer, R. B.; Geschwind, S.; Narayana-murti, V.; Devlin, G. E. *J. Appl. Phys.* **1979**, *50*, 1700.

(31) Marko, J. R.; Quirt, J. D. *Phys. Status Solidi B* **1974**, *64*, 325.

(32) Taira, N.; Wakeshima, M.; Hinatsu, Y. *J. Solid State Chem.* **1999**, *144*, 216.

(33) Cox, P. A.; Edgell, R. G.; Goodenough, J. B.; Kamnett, A.; Naishi, C. C. *J. Phys. C* **1983**, *16*, 6221.

(27) Cuffini, S. L.; Macagno, V. A.; Carbonio, R. E.; Melo, A.; Trollund, E.; Gautier, J. L. *J. Solid State Chem.* **1993**, *105*, 161.

(28) Goodenough, J. B. *Magnetism and the Chemical Bond*; Interscience: New York, 1963.

Accordingly, they could be classified as disordered Mott (Anderson–Mott) insulators. Electronic effects arising from a structural feature, specific to octahedrally coordinated d^0 transition-metal cations, place an upper limit on the ruthenium content that can be attained. We propose that to cross a metal–insulator transition in $\text{Na}_2\text{La}_2\text{Ti}_3\text{O}_{10}$ via substitution of the octahedral-site

cation, it will be important to attain high doping levels with a dopant atom very close in size to titanium and one containing a low number of outer d electrons. In this way the effects of disorder, correlation, and narrow bandwidth would be minimized.

CM9906452